Opto-Electronic Advances

Original Article

2020, Vol. 3, No. 4

DOI: 10.29026/oea.2020.190031

Passively Q-switched Tm/Ho composite laser

Haizhou Huang[1], Jinhui Li[1], Jing Deng[1,2], Yan Ge[1], Huagang Liu[3], Jianhong Huang[1], Wen Weng[1,2] and Wenxiong Lin[1]*

We explored Q-switching mechanism for the newly proposed Tm/Ho composite laser via developing a hybrid resonator for separating the intra-cavity Tm laser modulated by the saturable absorber (SA). With a Cr:ZnSe SA, successful passively Q-switching process with the maximum average output power of 474 mW and the shortest pulse width of 145 ns were obtained at the pulse repetition frequency of 7.14 kHz, where dual wavelength oscillation in both 2090 nm and 2097 nm was observed. This work provides an effective way for a direct laser diode (LD) pumped Q-switched Ho laser, which is compact and accessible. Furthermore, the current SA could be replaced by the 2D materials with broadband saturable absorption such as topological insulators or transition-metal dichalcogenides for seeking novel PQS lasers.

Keywords: Ho laser; Tm laser; Tm/Ho composite; passively Q-switched; Cr:ZnSe

Huang H Z, Li J H, Deng J, Ge Y, Liu H G et al. Passively Q-switched Tm/Ho composite laser. *Opto-Electron Adv* **3**, 190031 (2020).

Introduction

Within the transparent window of atmosphere and the strong absorption band of water, Ho lasers have a series of important applications in fields such as surgeries, mid-infrared super-continuum, and lidar systems[1–3], which have received more and more attentions. Particularly, pulsed Ho lasers with the wavelength around 2.1 μm are efficient pump sources for mid-infrared frequency conversion toward the 3~12 μm molecular fingerprint region[4] via optical parameter oscillation (OPO) or differential frequency generation (DFG)[5,6], owning to the wavelength farther away from absorption edge of the famous mid-infrared crystals ZPG and OP:GaAs than other Tm or Ho laser wavelengths[7].

Due to the lack of absorption band of Ho^{3+} at 800 nm, Ho lasers are commonly realized via the Tm, Ho co-doped mechanism[8] or intra-cavity pumping manner[9] for directly utilizing the mature AlGaAs LDs. However, the above lasers have limitations: attributing to the cooperative up-conversion process between the Tm^{3+} and Ho^{3+} ions, the Tm, Ho co-doped lasers should be cooled by cryogenic devices for Watt-level operation. Rigorous calibration between the separately cooled Tm-doped and Ho-doped gain media should be maintained for the intra-cavity pumped Ho lasers, which complicated the system setup. Hence, with the development of 1.9 μm lasers, such as Tm lasers or 1.9 μm LD, in-band pumping became a major way to realize Ho lasers for the past two decades[10–12]. However, the 1.9 μm pump sources are more expensive than common AlGaAs LDs and the setup is bulky especially when using the Tm lasers due to the cascade pumping scheme[13].

With the development of 2 μm saturable absorbers, such as 1D materials (single wall carbon nanotube and gold nanorod)[14,15], 2D materials (graphene, topological insulators, and ternary chalcogenides)[16–18], and transition metal ion-doped II-VI crystals (Cr^{2+}:ZnSe, Cr^{2+}:ZnS)[19,20], passively Q-switching (PQS) in 2 μm Tm-doped and Ho-doped lasers has become a hot topic, which is characterized by compactness, easy implementation, and cost-saving compared with the actively Q-switching (AQS) manners. Among the above SAs, Cr^{2+}:ZnSe/ZnS crystals were demonstrated to be robust for achieving higher

[1]Key Laboratory of Optoelectronic Materials Chemistry and Physics, Fujian Institute of Research on the Structure of Matter, Chinese Academy of Sciences, Fuzhou 350002, China; [2]University of Chinese Academy of Sciences, Beijing 100049, China; [3]Department of Electrical and Computer Engineering, National University of Singapore, 4 Engineering Drive 3, 117576, Singapore.

*Correspondence: W X Lin, E-mail: wxlin@fjirsm.ac.cn

Received: 31 July 2019; Accepted: 17 September 2019; Published: 20 April 2020

pulse energy and better PQS stability[19], owing to the mature crystal growth process with fewer defects. Although both PQS and AQS were well demonstrated in in-band pumped and Tm, Ho co-doped Ho lasers[12,21], Q-switching in intra-cavity pumped Ho lasers were limited due to the saturable effect in Ho-doped gain medium[22,23], which led to a disorder pulse burst and the failure in Q-switching.

Recently, via integrating the Tm-doped and Ho-doped gain medium into a single bulk structure, the Tm/Ho composite laser has been realized and demonstrated to meet the requirement of 2.1 μm lasers in compactness, accessibility, and robustness[24], which could be pumped by LDs with wavelength from 760 nm to 820 nm at broad room-temperatures[25]. However, pulse properties of such a Ho laser mechanism haven't been explored yet. On the other hand, saturable effect in both Tm-doped and Ho-doped regions of the composite gain medium will seriously challenge a successful Q-switching process due to the same resonant-pumping manner as the intra-cavity pumped Ho lasers. Hence, it is of significance to explore and realize Q-switching for the newly proposed Tm/Ho composite laser.

In this paper, crystalline Cr^{2+}:ZnSe crystal was selected as SA for exploring PQS properties of the Tm/Ho composite laser. Successful PQS process with the maximum output power of 474 mW and shortest pulse width of 145 ns was realized in a hybrid cavity structure, which could separate the intracavity Tm laser form Ho laser efficiently before modulated by the SA and in avoiding the cease in laser oscillation. The ideas here could also be adopted to realize PQS in the Tm/Ho composite lasers modulated by other SAs prepared with the 1D or 2D materials for seeking novel pulse Ho lasers.

Experimental setup

The schematic of the experiment is depicted in Fig. 1. A Tm/Ho:YAG crystal integrated via diffusion bonding the 3.5 at.% Tm:YAG and 0.6 at.% Ho:YAG crystals into a single bulk structure was served as the gain medium. The composite gain medium had a dimension of 3 mm×3 mm×14 mm with an 8 mm long Tm-doped region, which was wrapped by indium foil and mounted into a copper heat sink for water cooling at 16 ℃. A concave-plano cavity with a physical length of 60 mm was applied to make sure the smallest cavity mode size on the output coupler M2. M1 was a plano-concave mirror with radius of curvature of 100 mm, which was coated anti-refection (AR, T>97%) at 750–850 nm and high-reflection (HR, R>99.5%) at 1.9–2.2 μm. M2 was a plano-plano output coupler, which was HR at emission band of the Tm laser (R>99% at 1.9–2.02 μm) and had transmittance of 10% at Ho laser (T≈10% at 2.09–2.2 μm) respectively.

The Cr^{2+}:ZnSe SA with the dimension of 5 mm×5 mm×1.7 mm and initial transmittance of 92% at 2.1 μm was mounted into a copper heat sink and placed close to M2 for tight focusing operation[26]. For separating the intra-cavity Tm laser from modulated by the SA, a fused silica spectral filter F1 AR coated at 2.09–2.12 μm (T>95%) and HR coated at 1.9–2.02 μm (R>93%) were inserted inside the cavity to form a hybrid cavity structure. A fiber coupled 808 nm LD (NL-PPS50, Nligt Inc.) with a core diameter of 400 μm and numerical aperture of 0.22 was applied as the pump source. L1 and L2 are identical plano-convex mirrors with a focus length of 40 mm for forming a pump waist radius of 213 μm inside the composite gain medium, which was calculated by the ABCD matrix. M3 is a dichromatic mirror applied for filtering the Ho laser from the 800 nm pump light. The average output power was measured by an Ophir power meter (30(150)A-LP1-18, Ophire Inc.), and the lasing wavelength by a mid-IR spectrum analyzer (771A-IR, Bristol Instruments Inc.). Pulse properties of PQS composite Ho laser were analyzed by a 2 GHz bandwidth oscilloscope (MSO 2034, Tektronix Inc.) connected with an InGaAs detector (DET05D/M, Thorlabs Inc).

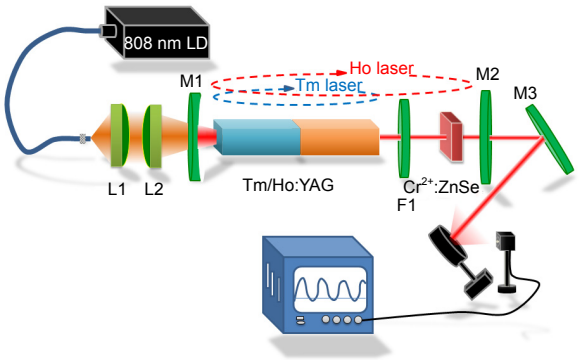

Fig. 1 | Layout of the PQS Tm/Ho composite laser.

Resonator for PQS Tm/Ho composite laser

According to the model for PQS lasers[27], key threshold criterion for the PQS process is

$$\alpha=\frac{\omega_s^2\sigma_{gs}}{\omega_c^2\sigma}>\frac{n_i/n_{th}}{n_i/n_{th}-1}\quad , \tag{1}$$

where σ_{gs} is ground state absorption cross section of the SA, σ is gain cross section of the Ho-doped region, ω_s and ω_c are cavity mode radii of the Ho laser on the composite

gain medium and the SA, respectively. n_i and n_{th} are dimensionless parameters meeting

$$\begin{cases} n_i = \ln(\frac{1}{T_0^2}) + \ln(\frac{1}{1-T_{OC}}) + L \\ n_{th} = \beta \ln(\frac{1}{T_0^2}) + \ln(\frac{1}{1-T_{OC}}) + L \end{cases}, \quad (2)$$

where T_0 is initial transmittance of the SA, T_{OC} is transmittance of the output coupler, L is the round-trip cavity loss, and β is ratio between σ_{gs} and the excited state absorption cross section σ_{es} of the SA.

In the concave-plano cavity for the Tm/Ho composite laser described by g parameters[25]

$$g_i = 1 - \frac{l_0}{R_i} - D(L_j + \frac{l_r}{2n})\left[1 - (L_i + \frac{l_r}{2n})\frac{1}{R_i}\right], \quad (3)$$

$$i, j = 1,2 \ \& \ i \neq j .$$

Cavity mode waist ω_s and ω_c can be written as

$$\omega_c = \omega_s \sqrt{\left[1 - \frac{1}{R_1}(l_1 + \frac{l_r}{2n})\right]^2 + \left[\frac{1}{l_e}(l_1 + \frac{l_r}{2n})\right]^2 \frac{g_1(1-g_1g_2)}{g_2}}, \quad (4)$$

$$\omega_s = \sqrt{\frac{\lambda_l l_e}{\pi}} \sqrt{\frac{g_2}{g_1(1-g_1g_2)}}, \quad (5)$$

where $l_e = l_1 + l_2 + \frac{l_r}{n} - D(l_1 + \frac{l_r}{2n})(l_2 + \frac{l_r}{2n})$

is the equivalent cavity length, l_0= 60 mm is length of the concave-plano cavity, R_i is curvature of radius of mirror M_i, l_i is distance between the gain medium and M_i. l_r, n, and D are the length, refractive index, and thermal lens of the composite gain medium.

As described in Ref.[28], D is proportional to the absorbed pump power P_{abs} and inverse proportional to the pump area as $D(P_{abs})=CP_{abs}/\omega_p^2$, where C is 8.2893 mm/W according to the calculation result in our previous work[25]. Hence, with other given cavity parameters, ω_s and ω_c are variables of P_{abs}, as shown in Figs. 2(a) and 2(b). As denoted in Fig. 3, peak gain cross section σ of the Ho-doped region is 1.4×10^{-20} cm^2. For the Cr^{2+}:ZnSe SA, σ_{gs} and σ_{es} are 1.3×10^{-19} cm^2 and 0.9×10^{-19} cm^2 respectively[29]. Inserting values of σ, σ_{gs}, and σ_{es} into Equation (2) and initializing L as 0.03, with the calculated ω_s and ω_c, evolution in the key parameter α in Equation (1) with P_{abs} is depicted in Fig. 2(c), where $\alpha_{th} = \frac{n_i}{n_{th}}\left(\frac{n_i}{n_{th}} - 1\right)^{-1}$ denotes the threshold value. As shown in Fig. 2(c), the higher curvature radius R_1 leads to the lager stable region and the smaller α, which is not suit for more stable PQS process according to threshold criterion. Although R_1=75 mm contributes for the largest cavity mode size in the gain medium and the smallest mode size in SA for tight focusing among R_1 of 75 mm, 100 mm and 200 mm, the shortest stable region denoted in Fig. 2(c) limits the achievable maximum output power for the PQS Ho laser. Therefore, M_1 with R_1 of 100 mm was applied in the following experiment, which brings moderate α and higher unstable threshold at approximately 6.5 W.

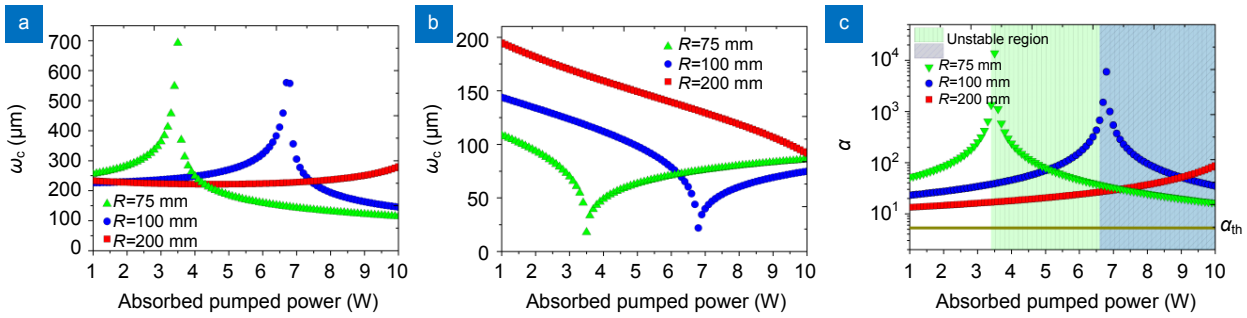

Fig. 2 | (**a**,**b**) Evolutions in cavity mode sizes ω_c and ω_s with the absorbed LD power P_{abs} at different M_1 curvature radii (R_1=75 mm, 100 mm and 200 mm); (**c**) Evolution in key parameter α with P_{abs} , where the colorful areas denote corresponding unstable regions (green for R_1=75 mm, blue for R_1=100 mm), α_{th} is $(n_i/n_{th})/(n_i/n_{th}-1)$ in Equation (1). Values of the parameters for the above calculation are summarized in Table 1.

Table 1 | Values of the parameters in Equations (1)–(5).

Parameter	Value	Parameter	Value	Parameter	Value
σ_{gs}	1.3×10^{-19} cm^2, Ref.[29]	λ	2122 nm	R_1	75 mm, 100 mm, 200 mm
σ	1.4×10^{-20} cm^2	L	0.03	l_1	8 mm
σ_{es}	0.9×10^{-19} cm^2, Ref.[29]	ω_p	213 μm	l_2	38 mm
C	8.2893 mm/W, Ref.[25]	T_{OC}	10%	n	1.82
T_0	92%	R_2	Infinity		

Results and discussion

The start of PQS

As shown in Fig. 3, emission bands of the intra-cavity Ho laser and Tm laser are within the designed initial transmittance curve of the SA. Due to the smaller gain cross section of Tm^{3+} ion compared with that of Ho^{3+} ion, oscillation in Tm laser was limited to sufficiently pump the Ho-doped region under both absorption losses from the Ho-doped region and the SA. Therefore, no oscillation in the PQS Tm/Ho composite laser was observed when directly inserted and adjusted the SA inside the laser cavity as normal PQS lasers.

As shown in Fig. 1, the spectral filter F1 was inserted into the cavity for preventing the Tm laser from being modulated and ceased by the SA and making sure the Ho laser oscillation. In the hybrid cavity consisted with M1, M2 and F1, characteristic pulse train of the free running Tm/Ho composite laser without SA is depicted in Fig. 4(a), which was irregular and unstable with time during the power scaling process. Stable PQS process occurred when inserting the SA into the hybrid cavity, where typical pulse train with the pulse repetition frequency (PRF) of 850 Hz and pulse width of 218 ns was shown in Fig. 4(b). Under the same absorbed LD power of 3.49 W, pulse train in Fig. 4(b) was regular with higher signal intensity compared with that in Fig. 4(a).

The laser properties

Before inserting the Cr:ZnSe SA inside the hybrid cavity, free running properties were measured first with the maximum output power of 667 mW and slope efficiency of 25.9% considering the absorbed LD power. As shown in Fig. 5(a), using the SA, the maximum average power decreased to be 474 mW at an absorbed LD power of 5.67 W with a slope efficiency of 20.3% and the lasing threshold increased from 3.04 W to 3.28 W due to the insertion loss from the SA. Beam quality of the PQS Ho laser at the maximum output power was measured to be with M_x^2=1.22 and M_y^2=1.15 in the horizontal and vertical directions, respectively, via using a beam quality analyzer (Nanomode scan, Ophire Inc.), where the corresponding beam profile with a concentric 3D beam shape at the beam waist was depicted in Fig. 5(b).

Lasing wavelength for the free-running Ho laser was stabilized at approximately 2122.2 nm during the power scaling process, which is the same as that from a simple plano-concave cavity in our previous work[25], where the characteristic spectrum at the maximum output power of 667 mW was shown in Fig. 6(a). During the PQS process,

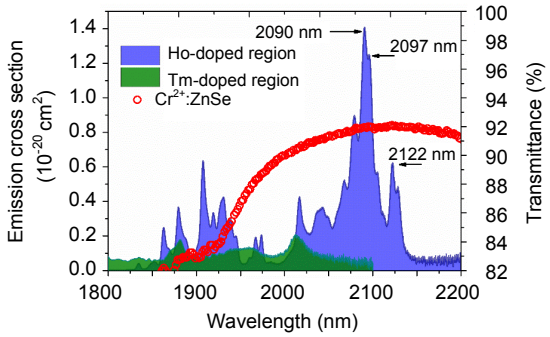

Fig. 3 | Emission cross section of the Tm-doped and Ho-doped regions and transmittance of the Cr:ZnSe SA.

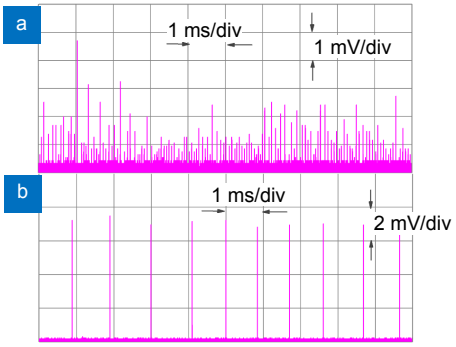

Fig. 4 | Comparison in pulse trains from the hybrid cavity before (a) and after (b) using the Cr^{2+}:ZnSe.

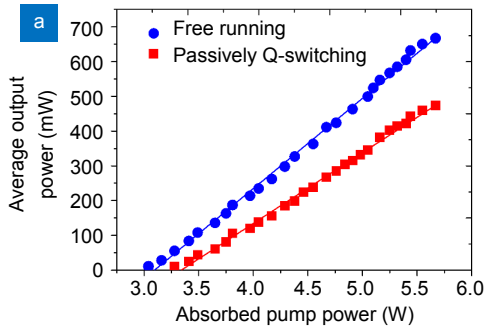

Fig. 5 | (**a**) Average output powers of the free-running Ho laser and PQS Ho laser versus absorbed pump power. (**b**) Beam profile of the PQS composite Ho laser at the maximum output power of 474 mW (Inset: 3D beam profile at the beam waist).

the wavelength at 2090 nm oscillated first (Fig. 6(b)) before scaling up the output power above 200 mW, where dual wavelength oscillation occurred at both 2090 nm and 2097 nm as shown in Fig. 6(c). Figure 6(d) illustrates the evolutions in Ho laser wavelengths at different output powers operating at free-running and PQS processes respectively. The measured Ho laser wavelengths were corresponding to the emission peaks of the Ho-doped region in Fig. 3, which switched from 2122 nm to shorter wavelengths due to the introduced cavity loss from the SA[30].

Evolution in PRF and pulse width for the PQS composite Ho laser were measured and depicted in Fig. 7. Increasing the average output power from 20 mW to 474 mW, PRF increased from 120 Hz to 7.14 kHz with the pulse width decreased from 229 ns to 145 ns correspondingly. Typical pulse train at the maximum PRF of 7.14 kHz was depicted in Fig. 8(a). Figure 8(b) shows the detail view of typical pulse profile from Fig. 8(a), which has a pulse width of 145 ns and corresponds to a pulse energy and a peak power of 66 μJ and 458 W, respectively.

Conclusions

In conclusion, we have demonstrated Q-switching properties of the recently proposed Tm/Ho composite laser, which met failure when following the traditional PQS manner due to the introduced modulation losses in both the intra-cavity Tm laser and Ho laser. A concave-plano hybrid resonator was designed for realizing a successful PQS process through filtering the intra-cavity Tm laser from Ho laser efficiently, where the maximum output power of 474 mW with a pulse width of 145 ns and a pulse energy of 66 μJ at PRF of 7.14 kHz was obtained. Through paving a way for achieving Q-switching in the Tm/Ho composite mechanism, this work tries to provide

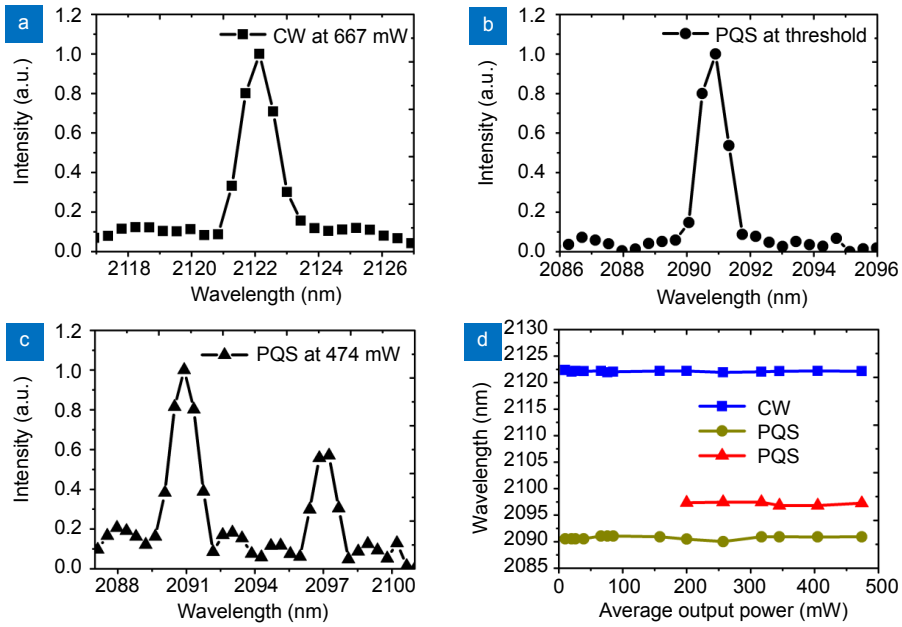

Fig. 6 | Wavelength properties of the Tm/Ho composite laser: (**a**) at the maximum free-running (CW) laser power; (**b**) at the threshold PQS laser power of 20 mW; (**c**) at the maximum PQS laser power; (**d**) the measured peak wavelengths at different average output power.

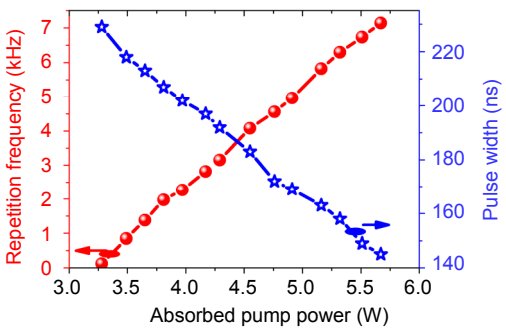

Fig. 7 | Evolutions in the pule repetition frequency and pulse width with the absorbed LD power.

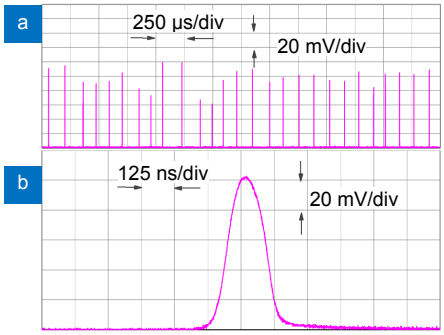

Fig. 8 | (**a**) Typical pules train with PRF of 7.14 kHz at the maximum PQS output power. (**b**) Detail view of the shortest pulse with a width of 145 ns at the maximum output power.

a compact and accessible pulse Ho laser which facilitates the direct use of common AlGaAs LDs. Moreover, the current SA can be replaced by the popular 2D materials, such as topological insulator, ternary chalcogenides, or graphene for exploring novel PQS Tm/Ho composite Ho lasers.

References

1. Hein S, Petzold R, Schoenthaler M, Wetterauer U, Miernik A. Thermal effects of Ho: YAG laser lithotripsy: real-time evaluation in an in vitro model. *World J Urol* **36**, 1469–1475 (2018).
2. Zhang J W, Fai Mak K, Nagl N, Seidel M, Bauer D et al. Multi-mW, few-cycle mid-infrared continuum spanning from 500 to 2250 cm^{-1}. *Light Sci Appl* **7**, 17180 (2018).
3. Mizutani K, Ishii S, Aoki M, Iwai H, Otsuka R et al. 2 μm Doppler wind lidar with a Tm:fiber-laser-pumped Ho:YLF laser. *Opt Lett* **43**, 202–205 (2018).
4. Schliesser A, Picque N, Hansch T W. Mid-infrared frequency combs. *Nat Photonics* **6**, 440–449 (2012).
5. Kanai T, Malevich P, Kangaparambil S S, Ishida K, Mizui M et al. Parametric amplification of 100 fs mid-infrared pulses in $ZnGeP_2$ driven by a Ho:YAG chirped-pulse amplifier. *Opt Lett* **42**, 683–686 (2017).
6. Hemming A, Richards J, Davidson A, Carmody N, Bennetts S et al. 99 W mid-IR operation of a ZGP OPO at 25% duty cycle. *Opt Express* **21**, 10062–10069 (2013).
7. Schunemann P G. New nonlinear crystals for the mid-infrared. In *Nonlinear Optics 2017* (Optical Society of America, 2017); http://doi.org/10.1364/NLO.2017.NTu2A.1.
8. Budni P A, Pomeranz L A, Lemons M L, Schunemann P G, Pollak T M et al. 10W Mid-IR holmium pumped $ZnGeP_2$ OPO. In *Advanced Solid State Lasers 1998* (Optical Society of America, 1998); http://doi.org/10.1364/ASSL.1998.FC1.
9. Bollig C, Hayward R A, Clarkson W A, Hanna D C, 2-W Ho:YAG laser intracavity pumped by a diode-pumped Tm:YAG laser. *Opt Lett* **23**, 1757–1759 (1998).
10. Budni P A, Pomeranz L A, Miller C A, Dygan B K, Lemons M L et al. CW and Q-switched Ho:YAG pumped by Tm:YALO. In *Advanced Solid State Lasers 1998* (Optical Society of America, 1998); http://doi.org/10.1364/ASSL.1998.ML4.
11. Chen H, Shen D Y, Zhang J, Yang H, Tang D Y et al. In-band pumped highly efficient Ho:YAG ceramic laser with 21 W output power at 2097 nm. *Opt Lett* **36**, 1575–1577 (2011).
12. Zhang Y X, Gao C Q, Wang Q, Na Q X, Zhang M et al. Single-frequency, injection-seeded Q-switched Ho:YAG ceramic laser pumped by a 1.91 μm fiber-coupled LD. *Opt Express* **24**, 27805–27811 (2016).
13. Lamrini S, Koopmann P, Schäfer M, Scholle K, Fuhrberg P. Directly diode-pumped high-energy Ho:YAG oscillator. *Opt Lett* **37**, 515–517 (2012).
14. Chernysheva M, Mou C B, Arif R, AlAraimi M, Rümmeli M et al. High power Q-switched thulium doped fibre laser using carbon nanotube polymer composite saturable absorber. *Sci Rep* **6**, 24220 (2016).
15. Huang H T, Li M, Liu P, Jin L, Wang H et al. Gold nanorods as the saturable absorber for a diode-pumped nanosecond *Q*-switched 2 μm solid-state laser. *Opt Lett* **41**, 2700–2703 (2016).
16. Zhao T, Wang Y, Chen H, Shen D Y. Graphene passively Q-switched Ho:YAG ceramic laser. *Appl Phys B* **116**, 947–950 (2014).
17. Liu X, Yang K, Zhao S, Li T, Qiao W et al. High-power passively *Q*-switched 2 μm all-solid-state laser based on a Bi_2Te_3 saturable absorber. *Photonics Res* **5**, 461–466 (2017).
18. Yan B Z, Zhang B T, He J L, Nie H K, Li G R et al. Ternary chalcogenide Ta_2NiS_5 as a saturable absorber for a 1.9 μm passively Q-switched bulk laser. *Opt Lett* **44**, 451–454 (2019).
19. Cole B, Goldberg L. Highly efficient passively *Q*-switched Tm:YAP laser using a Cr:ZnS saturable absorber. *Opt Lett* **42**, 2259–2262 (2017).
20. Lan J L, Xu B, Zhang Y Z, Xu H Y, Cai Z P et al. Tunable and passively Q-switched laser operation of Tm:$CaYAlO_4$ between 1848 nm and 1876 nm. *Opt Laser Technol* **109**, 33–38 (2019).
21. Li L J, Yang X N, Zhou L, Xie W Q, Wang Y L et al. Active/passive *Q*-switching operation of 2 μm Tm,Ho:YAP laser with an acousto-optical *Q*-switch/MoS_2 saturable absorber mirror. *Photonics Res* **6**, 614–619 (2018).
22. Schellhorn M, Hirth A, Kieleck C. Ho:YAG laser intracavity pumped by a diode-pumped Tm:YLF laser. *Opt Lett* **28**, 1933–1935 (2003).
23. Yang X F, Huang H T, Shen D Y, Zhu H Y, Tang D Y. 2.1 μm Ho:LuAG ceramic laser intracavity pumped by a diode-pumped Tm:YAG laser. *Chin Opt Lett* **12**, 121405 (2014).
24. Huang H Z, Huang J H, Ge Y, Zheng H, Weng W et al. 2.1 μm composite Tm/Ho:YAG laser. *Opt Lett* **43**, 1271–1274 (2018).
25. Huang H Z, Deng J, Ge Y, Li J H, Huang J H et al. Direct 800 nm diode-pumped Holmium laser with broad pump wavelength range and temperature adaptability. *Opt Express* **27**, 13492–13502 (2019).
26. Huang Y J, Huang Y P, Chiang P Y, Liang H C, Su K W et al. High-power passively Q-switched Nd:YVO_4 UV laser at 355 nm. *Appl Phys B* **106**, 893–898 (2012).
27. Tuan P H, Chang C C, Chang F L, Lee C Y, Sung C L et al. Modelling end-pumped passively Q-switched Nd-doped crystal lasers: manifestation by a Nd:YVO_4/Cr^{4+}:YAG system with a concave-convex resonator. *Opt Express* **25**, 1710–1722 (2017).
28. Chang Y T, Huang Y P, Su K W, Chen Y F. Comparison of thermal lensing effects between single-end and double-end diffusion-bonded Nd:YVO_4 crystals for $^4F_{3/2}\rightarrow{}^4I_{11/2}$ and $^4F_{3/2}\rightarrow{}^4I_{13/2}$ transitions. *Opt Express* **16**, 21155–21160 (2008).
29. Podlipensky A V, Shcherbitsky V G, Kuleshov N V, Levchenko V I, Yakimovich V N et al. 1W continuous-wave laser generation and excited state absorption measurements in Cr^{2+}:ZnSe. In *Advanced Solid State Lasers 2000* (Optical Society of America, 2000); http://doi.org/10.1364/ASSL.2000.MC7.
30. Barnes N P, Amzajerdian F, Reichle D J, Carrion W A, Busch G E et al. Diode pumped Ho:YAG and Ho:LuAG lasers, Q-switching and second harmonic generation. *Appl Phys B* **103**, 57–66 (2011).

Acknowledgements

We are grateful for financial supports from National Key Research and Development Program of China (Grant No. 2017YFB1104500), Natural National Science Foundation of China (NSFC) (Grant No. 61875200), and China Postdoctoral Science Foundation (Grant No. 2018M642575)

Competing interests

The authors declare no competing financial interests.